

Limits to Measuring Rural Economic Activity and Household Well-being from Space: Evidence from China with Three Generations of Night-time Lights Sensors

John Gibson (University of Waikato)¹

Xiaoxuan Zhang (Henan University), Yi Jiang (Asian Development Bank),

Xi Li (Wuhan University), Haiyuan Wan (Beijing Normal University),

Weidong He (Beijing Normal University), Albert Park (Asian Development Bank)

Abstract

Satellite-detected night-time lights (NTL) data are often used as proxies for economic activity and household well-being in data-poor settings, yet their effectiveness—particularly in low-density rural areas—remains uncertain. We compare three generations of NTL sensors using data from rural China: the widely used Defence Meteorological Satellite Program (DMSP), the research-oriented VIIRS, and China’s third-generation Luojia-01 and SDGSAT-1 that have finer spatial resolution and evening overpass times better aligned with household activity. Using county-level data on GDP, fiscal revenues, and poverty status, and township-level poverty rates, electrification rates and average household incomes, we assess predictive performance of each sensor. Despite advances in spatial resolution and sensitivity, newer sensors do not consistently improve prediction accuracy. Rural economic activity—especially agriculture—appears poorly suited to remote measurement via NTL. These results caution against over-reliance on satellite data and support continued investment in surveys to more effectively monitor rural development and household well-being.

JEL Codes: C83, O18

Keywords: Data-poor environments, poverty, household well-being, night-time lights

¹ Corresponding author. Contact details: john.gibson@waikato.ac.nz, Economics Group, Waikato Management School, University of Waikato, Private Bag 3105, Hamilton 3240, New Zealand.

I. Introduction

Measuring economic activity and household well-being in rural areas of developing countries remains especially challenging. Survey-based approaches inform less than often realized; rural livelihoods are spatial autocorrelated (Gibson et al, 2011) and logistics of getting interviewers into rural areas makes clustered sampling the most practical approach. Thus rural survey data have more uncertainty than would be found in a simple random sample of similar size fielded on a population whose livelihoods correlate less strongly with their neighbors (Gibson, 2019). Also, surveys often lack consistency in methods over time and space (DeWeerd et al, 2020) with measurement errors especially in (self-)reported agricultural production data (Jerven and Johnston, 2015). Survey errors can spill over into national accounts data on rural sector activity, which also face other measurement constraints in developing countries (Angrist et al, 2021).

It is against this backdrop that data captured by Earth-observing satellites have been proposed as a viable alternative. For example, Burke et al (2022) suggest a single satellite image might be able to tell the story of a village's economic health. Prominent studies include Jean et al, 2016; Watmough et al, 2019; Lobell et al, 2020; and Yeh et al, 2020. Potential advantages of remote sensing approaches include comparability between countries irrespective of varying levels of statistical capacity, lower cost and higher frequency data available sooner, and the possibility to build up from pixel level to form estimates for spatial units below the level at which national accounts data or survey data are typically reported.²

There are several types of Earth-observation data but economists especially focus on satellite-detected night-time lights (NTL) to proxy for economic activity (Chen and Nordhaus, 2011; Henderson et al, 2012; Gibson et al, 2020) and household well-being (Bruederle and Hodler, 2018). For example, satellite-detected data on a village's lights at night are claimed to

² Survey-to-census imputation methods (e.g. Elbers et al, 2003) can facilitate construction of small-area welfare estimates (which now extend beyond expenditures and poverty to many other indicators, as noted in Dang et al, 2025) but temporal coverage is often limited by census infrequency.

allow inferences about village-level economic productivity (Burke et al, 2022); far more finely grained than traditional measurement allows. Yet there are emerging doubts over the universal usefulness of NTL data as a proxy. For example, NTL data seem to be a poor proxy for showing variation in economic activity over space in low-density rural areas of developing countries (Gibson et al, 2021). Relatedly, in a cross-country panel study, changes in NTL data did not positively correlate with changes in GDP in countries where agriculture and forestry had large shares of GDP (Keola et al, 2015). A failure of changes in NTL data to predict changes in indicators like employment and household expenditures is also seen at local levels in developing countries (Goldblatt et al, 2020; Asher et al, 2021).

It may be that rural economic activity, especially agriculture, is intrinsically unsuited to remote measurement by NTL. For example, Gibson and Boe-Gibson (2021) find changes in county-level agricultural GDP and in NTL data in the United States are unrelated, yet activity changes in other sectors significantly co-vary with changes in lights. Also, the cross-sectional lights-GDP relationship in the primary sector is less than one-fifth as strong as for other sectors. Bluhm and McCord (2022) use subnational data from six countries (including the US) and find the GDP–lights elasticity is especially low for agricultural GDP—and that this cannot be all due to measurement error.³ Taken together, these studies point to a structural limitation: much rural activity is too weakly illuminated or too dispersed for observations from space to provide reliable evidence on household well-being.

Alternatively, these unpromising results for the rural sector may be due to studies using data from first-generation NTL sensors meant to detect clouds for short-term Air Force weather forecasts—the Defense Meteorological Satellite Program (DMSP)—rather than for long-run monitoring of dimly-lit and dispersed rural economic activity. At least two technical limitations

³ Khachiyan et al (2022) use daytime imagery (from Landsat) to predict income and population for micro-grids with far greater accuracy than they achieve when using DMSP NTL data. However, their study is restricted to urbanized US census blocks and does not use the more accurate second- or third-generation NTL data. So it is still an open question as to whether rural economic activity is also hard to proxy with daytime imagery.

of first-generation sensors are salient: coarse spatial resolution and limited dynamic range. The DMSP data are presented as a continuous surface varying smoothly over space, in raster format for 30 arc-second grid cells that are ca. 1 km^2 at the equator (getting smaller at higher latitudes), but spatial resolution of the sensors recording lights is far coarser.⁴ The clearest account is by Elvidge et al (2013), who show a pixel footprint (Ground Instantaneous Field of View, the area on Earth's surface sensed at a single moment in time) of 25 km^2 ($5 \text{ km} \times 5 \text{ km}$), when satellites are directly overhead (near-nadir observations). Pixel footprints expand away from the nadir due to viewing the Earth at an angle, by up to 2.4-fold at 750 km off-nadir (Falchi and Cinzano, 1998), beyond where NOAA scientists stop using images as they are too blurred. So the pixel footprints are between $25\text{--}60 \text{ km}^2$ and lights attributed to a particular point may be from several kilometres away (Abrahams et al, 2018)—this may not matter for national or provincial level analysis but should matter at village or household level. In contrast, second generation sensors from NASA's research-oriented VIIRS (Visible Infrared Imaging Radiometer Suite) have pixel footprints of $\sim 0.6 \text{ km}^2$ with in-built compensation for the off-nadir expansion. Third-generation NTL sensors from China, LuoJia-01 and SDGSAT-1, have pixel footprints of ca. 0.02 km^2 and below, so there have been orders of magnitude improvements in spatial resolution over time.

The dynamic range of radiance values (brightness levels) that the DMSP sensor detects and accurately represents—from the darkest to the brightest areas—covers only two orders of magnitude while second- and third-generation sensors cover at least seven orders of magnitude (Nechaev et al, 2021). Hence, DMSP gets top-coded in brightly lit areas, especially in the lunar cycle phase when raw moonlight is insufficient to illuminate cloud tops so sensor magnification is amplified, and gets bottom-coded if weakly illuminated areas are treated as unlit. Top-coding

⁴ Studies in economics using DMSP data have ignored this difference, instead suggesting that *measurement* of luminosity occurs at the 1 km^2 level. Examples of this claim, and visual evidence that it is not true, are provided by Gibson et al (2025) while a careful distinction between resolution of the output grid versus that of the sensor is in Rogers et al (2023). Some remote sensing studies suggest DMSP spatial resolution of $2.7 \text{ km} \times 2.7 \text{ km}$ but this seems to account only for the pixel averaging into 5×5 blocks (needed due to onboard data storage limits) and does not account for the random geolocation errors of $2.9 \pm 1.0 \text{ km}$ that are discussed by Tuttle et al (2013).

of DMSP receives more attention in economics (Bluhm and Krause, 2022) but bottom-coding (false zeros) is the more likely problem in rural areas. For example, Chen and Nordhaus (2015) find that for 600 cells (of $1^\circ \times 1^\circ$) in Africa with populations below 10,000 but all illuminated according to VIIRS, 72% showed no light according to DMSP. Likewise, 77% of counties in North Korea appearing to be entirely dark in DMSP images were illuminated according to VIIRS data (Kim et al, 2024). So misdetection of weakly illuminated areas is a major problem.

This paper frames the issue as a horse race between two explanations: (1) NTL has underperformed in rural settings because earlier studies relied on first-generation sensors that were too coarse and insensitive, if studies use second- and third-generation sensors designed to measure on-the-ground activity there may be better proxying of rural economic activity and household well-being; versus (2) rural livelihoods, especially in agriculture, generate too little night-time luminosity for any sensor to capture reliably. We provide a large-scale comparative test of these explanations using three generations of NTL sensors in rural China, benchmarking DMSP, VIIRS, and LuoJia-01/SDGSAT-1 against county-level primary GDP, fiscal revenues, and poverty indicators, and also against township-level poverty rates, electrification rates, and average household incomes. Even with major advances across sensor generations—including finer spatial resolution, improved detection of low-light emissions, and more suitable overpass times (around 9:30pm for LuoJia-01/SDGSAT-1 that better aligns with household activity)—newer systems do not consistently improve predictions of rural economic activity or household well-being. These findings matter not just for academic debates about measurement, but also for the way governments and donors allocate scarce resources: if enthusiasm for satellite-based remote measurement approaches outpaces actual performance, required investment in survey innovations that are designed to better capture rural realities may be endangered.

The next section describes properties of the three generations of NTL sensors used in our analysis, along with ground-truthing exercises to confirm, consistent with their theoretical

design, that LuoJia-01 and SDGSAT-1 can detect village-level features in China less visible to the earlier generation sensors. Section III sets out our China-wide sample of 1,460 rural counties and the township-level census data from 13 of these counties, covering all households in 265 townships, together with the indicators used to compare predictive performance across sensors. Section IV presents the main results, benchmarking each sensor against county-level measures of primary sector GDP, poverty status, and fiscal revenues, and against township-level data on poverty, electrification, and average household incomes. Section V discusses the findings and our conclusions in Section VI consider the measurement implications.

II. The Competing Sensors

In total we use five sources of night-time lights data: DSMP, two competing VIIRS platforms (VNL from the Earth Observation Group of the Colorado School of Mines, and Black Marble from NASA), LuoJia-01 and SDGSAT-1. We are not able to align all five sources in the same year, limiting our attention to a cross-sectional analysis.⁵ Specifically, SDGSAT-1 only began in November 2021 while the DMSP extension series (Ghosh et al 2021) ended the next month, so comparing first- and third-generation sensors in 2021 would be for fewer than five nights of observations (SDGSAT-1 has a revisit time of every 11 days). Instead, we mainly work with data from 2018—helpfully being before the COVID-19 disruptions—supplementing analyses with some SDGSAT-1 readings from 2021. There is an overlap of more than six months for DMSP and LuoJia-01 in 2018, plus annual data from the second-generation VIIRS sensors.

Table 1 has a summary of relevant attributes of the five data products. A visualization that compares resolution of the pixel footprints at the nadir is given in Figure 1, inspired by a

⁵ A consistent theme in the literature is that NTL data far better predict cross-sectional differences in economic activity than time-series changes in activity (Nordhaus and Chen, 2015; Zhang and Gibson, 2022; Chen, 2025) and the same is true for predicting indicators derived from household surveys (Goldblatt et al, 2020; Asher et al, 2021). So our comparison across sensor generations is in the context where NTL data appear to work best. In future, comparison of second- and third-generation sensors for studying changes in household well-being could use the Chinese Family Panel Studies, which gathered data in 2022 and 2024, but the 2024 data are not available until 2026 (highlighting the timeliness advantage of the Earth-observation approach to monitoring well-being).

similar figure in Elvidge et al (2013) for DMSP and VIIRS (but not third-generation sensors). There is over a 1000-fold difference in the size of the pixel footprints for first-generation versus third-generation sensors; the gap is even larger off-nadir due to the footprint expansion coming from the angular viewing effect. Such effects are naturally more limited for the third-generation sensors, which orbit closer to Earth (e.g. 505 km for SDGSAT-1 vs 850 km for DMSP) and have a far smaller swath (e.g. 250 km for Luojia-01 vs 3000 km for DMSP).

We use averages of DMSP annual composites for the two satellites (F15 and F16) that provided data in 2018.⁶ The composites are processed by the Earth Observation Group (EOG) to exclude ephemeral lights from fires and flaring and also exclude any pixel-nights affected by clouds, moonlight, sunlight and other glare. The observation time is ca. 3.30am, compared to the usually reported 8.30pm observation time for the DMSP time-series that ended in 2013.⁷ The data are 6-bit digital numbers (DN) ranging from 0–63 (higher for more light), presented on a 30 arc-second output grid.

We use two types of annual VIIRS data for 2018: VIIRS Night Light (VNL) from EOG and Black Marble (BM) from NASA. Their common source is the Suomi/NPP satellite that has been observing NTL at 1.30am since 2012 but they are processed differently. The VNL annual composites are built from monthly cloud-free radiance averages, initially filtered to remove extraneous features such as fires and aurora and the resulting rough composites have further outlier removal procedures applied and a stray-light correction (Elvidge et al, 2021). The data are in units of nano Watts per square centimetre per steradian ($\text{nW}/\text{cm}^2/\text{sr}$), on a 15 arc-second output grid (ca. 0.5×0.4 km at China's latitude). The Black Marble data are corrected for atmospheric, terrain, vegetation, snow, lunar, and stray light effects on radiance values (Román

⁶ These data are available from: <https://eogdata.mines.edu/products/dmsp/#download>. Results using data from F15 and F16 separately are very similar to the results using their averages, and are available from the authors.

⁷ Unstable orbits for DMSP satellites meant they observed the earth earlier as they aged, so Ghosh et al (2021) extended the time series past 2013 by switching from late afternoon observations, which were not useful for measuring luminosity, to the corresponding pre-dawn observations (given the 12 hour revisit time).

et al., 2018). The BM data differ from VNL data in four ways: reporting is with 16-bit precision (n=65,536 values) rather than 14-bit (n=16,384 values), users have a choice of near-nadir, off-nadir, or all-angles composites, the data for snow-free and snow-covered nights are provided separately, and a mosaic of 648 tiles covers the Earth's surface (while VNL provides a single global composite).⁸ We form a weighted average of snow-free and snow-covered data (BMwa), using the share of snow-free nights as weights; this has been shown to better predict China's annual economic activity than snow-free data alone (Zhang and Gibson, 2022).

The LuoJia-01 satellite was developed by Wuhan University and began providing data in June 2018. Spatial resolution is finer than first- and second-generation sensors, with a pixel footprint of 130 metres on the side (ca. 0.02 km²) at the nadir. The 14-bit digital numbers are presented on a 4.44 arc-second output grid (ca. 0.1×0.1 km at China's latitude). LuoJia-01 better detects feeble lights than do earlier generation sensors, such as VIIRS, (Li et al., 2019), which should matter for rural areas. In terms of observing household economic activity, the local observation time is ca. 9.30pm, as opposed to 1.30am (BM and VNL) and 3.30am (DMSP).⁹

The most recent third-generation sensor is SDGSAT-1, launched in November 2021 by the International Research Center of Big Data for Sustainable Development Goals (CBAS), the Chinese Academy of Sciences. It carries the Glimmer Imager, which provides panchromatic nighttime data at 10 m resolution and multispectral data (red, green, blue) at 40 m resolution, giving a pixel footprint at nadir of 0.0001 km². This sensor flies closest to Earth of any NTL sensor, and the swath width of only 300 km (one-tenth that of DMSP) further limits any angular viewing effects. The data are provided as 16-bit digital numbers. The overpass time of around 9:00 pm aligns more closely to timing of peak household activity compared to earlier sensors.

⁸ The VNL data are available from: https://eogdata.mines.edu/nighttime_light/annual/v21/ and the Black Marble data from: <https://ladsweb.modaps.eosdis.nasa.gov/archive/allData/5000/VNP46A4/>.

⁹ The data are available to download from the High-Resolution Earth Observation System of the Hubei Data and Application Center (<http://59.175.109.173:8888/app/login.html>).

2.1 Illustrating Spatial Resolution Using Ground-truthing Exercises in Rural China

To illustrate how third-generation sensors capture features in China's rural villages that are not seen with earlier generation sensors we took some first-hand observations to provide a limited ground-truthing exercise in two villages in central China: Xiyang village of Mianchi county Henan province, and Sidi village of Tongguan county Shaanxi province. In each village, the second author went to the main crossroads in the village in late 2021 and then chose the axis (east-west or north-south) with the larger road, and travelled along that road taking photographs at 1 km intervals out to a 3 km perimeter (i.e., providing a simple transect). We then compared satellite-detected luminosity data for these points with what was seen on the ground. We used 2021 data from SDGSAT-1 and 2018 data for the other sensors; with the relatively static nature of built-up area in these villages the photographs from 2021 should also reasonably align with what was the on-the-ground situation in 2018.

In Xiyang village, at the 3 km marks there were no buildings and the land was covered in crops (and an unlit pathway), the 2km marks had sparsely scattered buildings, and the 1 km marks inwards had paved surfaces and built-up area with two-storey buildings (Figure 2a). The third-generation sensors reflected this transect very closely; at 3 km NTL values were just 7% of the value at the crossroads, at 2 km they were 15-35% of the peak value, and 41-86% at the 1 km marks (with SDGSAT-1 declining faster away from the village centre than LuoJia-01). The first- and second-generation sensors showed far less differentiation; luminosity at the 3 km (2 km) marks was 67% (79%) of the value given for the output cell corresponding to the village crossroads, with both the DMSP and BMwa data.

In Sidi village (Figure 2b), third-generation sensors had NTL values at the crossroads that were 12-times higher, on average, than the values at the 3 km marks. In contrast, the DMSP luminosity value at the crossroads were just 1.4-times as high as at the 3 km marks; in other words, DMSP barely detected the village compared to the surrounding area due to the inherent

smoothing that occurs with a large pixel footprint. One concern with this comparison may be the time of detection; ca. 3.30am for DMSP versus 9pm for LuoJia-01 and SDGSAT-1. Yet the same flatness along the transect shows up if data from DMSP satellite F18 in 2013 are used, with the value at the crossroads only twice as high as at the 3 km marks (compared to a 12-fold difference using the third-generation sensors)—notably DMSP overpass time was ca. 8.30pm in 2013. The two-fold difference between luminosity at the crossroads and the 3 km marks is also what second-generation BMwa data suggest for Sidi village—slightly more sensitive to differences in lighting along the transect than in the first village but still with lights appearing to come from unlit fields at the 3 km marks, yet the most sensitive SDGSAT-1 readings show zero luminosity that far out from the village centre. Overall, this on-the-ground evidence shows how the earlier generation sensors may distort understanding of exactly where built-up area is located and insufficiently distinguish this built-up area from the agricultural hinterland.

2.2 Prior Literature on Performance of the Sensors

The properties of the sensors outlined in Table 1 (and pixel footprints shown in Figure 1) lead us to expect that data from a first-generation sensor like DMSP will less accurately predict rural economic activity and poverty than second-generation data from VNL or Black Marble, and likewise third-generation sensors like LuoJia-01 and SDGSAT-1 should perform better than data from VIIRS. To date, the literature has not compared all three generations of sensors at once, but the partial rankings are suggestive. For example, an early cross-sectional study found VIIRS data better predict county-level GDP in China than do DMSP data (Shi et al, 2014) and the same pattern was found at provincial and prefectural level (Dai et al, 2017). A comparison for a wider set of socio-economic indicators found VIIRS data were generally a better proxy although the later observation time (compared to the pre-2014 DMSP data) lowered the correlations for some indicators (Jing et al, 2015). A feature of DMSP is that measurement errors are spatially mean-reverting (Gibson, 2021), so their effects become more apparent when

proxying for economic activity of smaller, lower-level, administrative units; in contrast, DMSP does less badly in predicting for more aggregated units, such as provinces, because the effects of mean-reverting errors are mitigated by aggregation (Gibson et al, 2021).

Comparisons of LuoJia-01 to earlier generation sensors are mostly with VIIRS, as the DMSP data for 2018 only recently became available (Ghosh et al, 2021). For example, when modelling socio-economic parameters in eastern and central regions of China, Zhang et al (2019) found LuoJia-01 data out-performed the equivalent VIIRS data. Liu et al (2020) created a 20-factor multi-dimensional economic development index for counties in three provinces (Hubei, Hunan and Jiangxi) and found LuoJia-01 data had better fit with this index in a random forest model than did VIIRS data. Lin et al (2022) found that there was a slight improvement over VIIRS when using LuoJia-01 data in a random forests model for estimating the poverty status of 126 counties (and districts) in Chongqing and Guizhou in China.

With the emergence of SDGSAT-1, data from this new third-generation sensor are now compared to data from earlier sensors, but mostly focused on urban research (Dong et al, 2025). For example, for the five leading urban agglomerations in China data from SDGSAT-1 were better than VIIRS and DMSP data, for extracting built-up area (Li et al, 2023) and a study just for Shanghai reached the same conclusion when comparing SDGSAT-1 to VIIRS (Xie et al, 2024). The rural evidence is more fragmentary and less promising. For example, a household survey of economic well-being in Bazhou county-level city of Hebei province found village- and township-level well-being only weakly related to either total or average levels of NTL, as detected by SDGSAT-1 (Jiang et al, 2025). At the county-level in Guangdong province, Chen et al. (2025) used SDGSAT-1 and VIIRS to predict a Multidimensional Poverty Index (MPI), and SDGSAT-1 gave only a minor improvement in the predictions, reinforcing the view that third-generation sensor resolution gains alone do not necessarily make much difference in rural poverty prediction.

III. Estimation Sample, Selected Indicators and Comparison Procedures

3.1 Sample

For the main analysis we selected all rural counties in China for testing if NTL data from newer sensors more accurately predict rural economic activity and household well-being compared to the NTL data from earlier generation sensors. From all third-level sub-national units in China's 2020 census ($n=2848$) we first removed districts (these are the urban cores of cities). Next we removed county-level cities; the primary sector share of GDP in such places averages just 1.3% (and is no higher in county-level cities than in districts). This left us with a sample of $n=1460$. This sample is predominantly counties ($n=1415$) but in the parts of China not administered as prefectures (as the second-level unit) the other third-level units may be banners and special areas ($n=45$).¹⁰ We refer to all of these as counties for simplicity. In this sample, the GDP share from the primary sector averages 37%. The sample selection flowchart is given in Figure 1 of Appendix A, while the map showing the areas we cover is in Figure 3.

Counties are the most commonly used administrative unit in prior studies using NTL data for poverty predictions in China (Xu et al, 2021; Chen et al, 2025). However, the median area of counties in our sample is 2200 km²—an area that may be too large for the advantages of finer resolution third-generation sensors to perhaps improve poverty predictions. So we also obtained sub-county data for 13 counties in the sample (the red outlines in Figure 3) and used these to calculate well-being indicators for all 265 townships in these counties.¹¹ The median township in this sample covers 74 km²—a smaller area than in some well-cited prior studies relating NTL data to household well-being (e.g. Bruederle and Hodler, 2018).¹²

¹⁰ For non-county and non-city areas (e.g. banners), if in doubt about suitability for inclusion the primary sector share of GDP was used as a criteria. The excluded areas were especially coal mining areas from Inner Mongolia.

¹¹ These 13 counties are all east of the Hu line that runs from western Yunnan to northern Heilongjiang; to the west of this line almost three-fifths of China's land area is home to just 6% of the population. So these counties represent where the population is located, and the absence of any in western or northeastern areas reflects a very low population density in such places; an imbalance not easily conveyed with the map.

¹² They used average NTL values in a 5 km buffer around the reported DHS EA coordinates; if coordinates were exact this would cover an area of 79 km². However, reported coordinates are displaced up to 5 km in rural areas, to anonymize surveyed communities, whereas we have the actual boundaries for the townships used here.

These sub-county data are from the National Poverty Alleviation and Development Information System (NPADIS); a component of China’s targeted poverty alleviation strategy launched in 2013. This database covers the entire population at risk of poverty in China and is built up from annual censuses covering all rural households in targeted counties, conducted by local officers in each village. The list of Identified Poor Households was adjusted each year after 2013, based partly on these censuses, and we have data from the 2017 census, which is the latest available (and in the adjacent year to the 2018 luminosity data). Notably, these census data provide a comprehensive record that can be aggregated to the township level as a complete enumeration rather than a sample. We are aware of one prior published study using these data (Zhang et al, 2023), but just for one county rather than the 13 counties that we have data for.

3.2 *Indicators of Rural Economic Activity and Household Well-being*

We use primary sector GDP (in billions of Yuan, CNY) for each county in 2018, from the 2019 edition of the *China Statistical Yearbook* (county-level), known in Chinese as *Zhongguo Xianyu Tongji Nianjian*.¹³ The same yearbook also provides our second indicator of economic activity (and of ability to fund local public goods that may affect household well-being), which is the fiscal revenue generated in each county. Our third indicator is a binary variable for the poverty status of each county, which is determined by the State Council Leading Group Office of Poverty Alleviation and Development (LGOPAD). The basis of this classification was that a group of $n=832$ rural counties had been defined as poverty-stricken in 2013 and thereafter the National Bureau of Statistics used an annual National Rural Poverty Monitoring survey to update the progress of these counties in moving out of poverty.¹⁴ We use the situation as it was

¹³ Such disaggregated GDP data, at the third sub-national level, are rarely available; while the United States also reports county-level GDP, other large countries like India and Indonesia only report at the second sub-national (district) level, and Eurostat only reports down to the NUTS2 level, which is aggregations of counties in some countries (e.g., the UK) and refers to the provincial level in others.

¹⁴ Earlier classifications of counties as poverty stricken were found to have targeting errors with respect to per capita income (Park et al, 2002). A switch to village-level targeting (the Integrated Village Development Program) was made in 2001. This intervening regime, and the fact that the number of poverty counties in 2013 exceeded the number of poor counties from the pre-2001 regime, means that the earlier criticism of targeting errors for the pre-2001 poor county designation does not automatically apply to the post-2013 classification. In

at the beginning of 2018, when $n=679$ counties were still defined as poverty stricken across all of China, with $n=578$ of these counties in our sample.

At the township level we calculated three indicators from the unit record data for 2017: the poverty rate, the electrification rate, and average per capita net income. The poverty rate is the ratio of the number of persons living in Identified Poor Households (IPH) to the township population. The IPH status is primarily income-based but housing, education, and health also factor into the classification; for example, living in dilapidated dwellings gives IPH status even if per capita net income exceeds the poverty line. Conversely, some forms of employment (e.g. as a civil servant) and ownership of expensive assets or urban real estate lead to exclusion from the IPH list. Moreover, preliminary IPH status is first publicly announced within the village and is then subjected to rigorous multi-level verification, undergoing successive reviews at the town, county, and higher level LGOPAD offices before being included in the database.

3.3 *Luminosity Indicators*

We use data from the competing sensors to form three sets of luminosity variables, all of which are found in applied economics studies using NTL data. The first is the sum of lights by county or township, which is the product of lit area and average brightness within lit areas; previous studies relating NTL to poverty suggest this is a sufficient statistic for the relevant variation (Gibson et al, 2017; Gibson et al, 2023). Moreover, non-nested tests show that the sum of lights outperforms other luminosity variables for predicting China's county-level GDP (Zhang and Gibson, 2022). We also use the sum of radiance divided by county area, following Henderson et al (2012) and Castelló-Climent et al (2018), even though GDP is rarely normalized by area. Third, we use the share of pixels in a county that are illuminated; the inverse of this measure, or relatedly the share of the population living in unlit rural areas, is used in studies of rural

support of this claim, we show below that the current designation reflects environmental influences (such as elevation and temperature) that were previously neglected in the poor county designation (Olivia et al, 2011). Hence it is reasonable to consider this new poor county classification as a break from the past.

poverty by Smith and Wills (2018) and Maldonado (2023). Summary statistics for the outcome measures and for the sum of lights (at county-level and township-level) are given in Table 1 of Appendix A.

3.4 *Other Predictors*

The machine learning models used in the literature to predict rural poverty often draw upon a large set of predictors and so we want to evaluate the NTL data both as unconditional predictors and also when covariates are included. We use eight covariates that control for environmental conditions and land cover: the average elevation, precipitation, and temperature, and then the proportion of each area (i.e., county or township) that is cultivated, forested, urbanized, village settlement, or industrial and infrastructural—where these five land cover variables are derived from daytime Landsat images (Song and Deng, 2017).

For the land cover categories that refer to built-up area, there are varying relationships with luminosity that are shown by all four NTL data sources (Table 2). In particular, village built-up area has a far smaller effect on the county sum of lights than from similarly sized urban area or industrial and infrastructural area. Averaging across the four NTL data sources, for each 1 km² of village built-up area the sum of lights is (unconditionally) 0.7 percent higher, while it is 3.8 (1.6) percent higher per 1 km² of urban (industrial and infrastructure) area. With all three types of built-up area in the same regression, county lights are 0.3 percent higher per km² of village area, on average and holding the other types of built-up area constant; 2.5% higher per km² of urban area (conditional on the other types of built-up area) and 1.4% higher per km² of industrial and infrastructural area. For all four sources of NTL data, we would reject the hypothesis that village built-up area has the same effect on the county luminosity totals as do the other two types of built-up area. The results in Table 2 show that NTL data are far more responsive to differences in urban area, or industrial and infrastructural area, than they are to variations in built-up area of villages.

3.5 Empirical Specification

We relate each economic activity or well-being indicator to each luminosity indicator, using estimates from each sensor separately, with the following regression:

$$\ln(\text{activity or wellbeing indicator})_i = \alpha + \beta \ln(\text{luminosity indicator})_i + \varepsilon_i \quad (1)$$

where we also include control variables in some of these regressions. For one outcome (county poverty status) and for one luminosity indicator (the share of illuminated pixels) we cannot take logarithms due to possible presence of zeros and so results in those cases use standardized variables. We place no causal interpretation on equation (1), which is just one way to find the best predictors amongst the set of NTL variables.

IV. Results

4.1 County-level results

The results of estimating equation (1) with county-level data are shown in Table 3 for primary sector GDP, in Table 4 for poverty status, and in Table 5 for fiscal revenue. In terms of the way that the NTL data are used, lights normalized by area or the percentage of illuminated pixels is almost never as predictive as just using the sum of lights. For example, for the two continuous outcome measures (primary sector GDP and fiscal revenue), just two out of the 48 sets of results reported in Tables 3 and 5 are examples where the best-fitting specifications are using something other than the sum of lights. For county-level poverty status, there is almost no difference in predictive power between the three ways of using the NTL data when the control variables are included, while in the regressions without control variables lights normalized by area is a slightly better fitting specification, but with adjusted R^2 values that never exceed 0.14, showing the overall weakness of the predictive power.

Irrespective of whether we control for land cover and environmental factors, or simply look at unconditional predictions, there is no gradient whereby data from the newer and better sensors lead to either larger estimated elasticities of the economic activity or welfare indicators

with respect to luminosity, or to higher R^2 values for the prediction equations. A visualization of this lack of gradient, whereby data products coming from newer generation sensors give no stronger predictions, is shown in Figure 4, for the sum of lights (as the best-fitting specification) and with the sign of the elasticity of county poverty status with respect to lights reversed so the patterns are clearer.¹⁵ When control variables are included, the adjusted R^2 values are almost flat across the three generations of sensors, in fact, for the equations for county fiscal revenue the R^2 values are slightly lower when using data from the third generation Luojia-01 sensor than from the first generation DMSP (and this same pattern, of the Luojia-01 data providing weaker predictions than the DMSP data is seen for all three outcomes in the regressions without control variables). In other words, it does not seem that the data from newer sensors with finer spatial resolution and greater sensitivity to weak lights do a better job of predicting primary sector economic activity, poverty status or fiscal revenue for these rural counties.

4.1.1 Machine Learning Results

The results reported thus far have used traditional regression approaches but much of the recent literature using satellite imagery for poverty predictions is based on machine learning (Hall et al, 2023). To ensure that our comparisons of the predictive power of data derived from different generations of satellite remote sensing systems are salient to this recent literature we also used a random forests (RF) algorithm (which is a form of supervised machine learning) to predict the county-level poverty status. This is an ensemble learning method that combines multiple decision trees for solving classification and regression problems (Breiman, 2001). Recent studies using luminosity data in Asia find the RF method has the best predictive performance (Puttanapong et al, 2023; Fenz et al, 2024). A key feature for our application is that the RF method is quite suitable for the task of assessing variable importance, when compared to other frequently used machine learning methods (Grömping, 2015).

¹⁵ Confidence intervals are not shown on the charts, to reduce clutter. Standard errors are reported in the tables.

To obtain the RF predictions we used the randomForest package in R which allows us to have enough decision trees to generate them with randomness when building the forest. Each of the individual trees is built independently with a subset of the entire training dataset, where this subset is drawn using bootstrap sampling with replacement. Two-thirds of the instances in the bootstrap samples were used to train the individual trees, while the rest were used as testing data to evaluate the final RF classifier. The instances used for training the individual trees are referred to as in-bag instances, and the instances for testing are out-of-bag instances. In order to achieve robust results, the processing of building and selecting the final RF model is repeated 1000 times. This ensured that the RF model can include different sets of predictor variables in the training and testing samples, so that stable and reliable results are produced.

We first used just the four NTL predictors (the log of the sum of lights from DMSP, VNL, BM and Luojia-01) and then subsequently included the eight environmental factors and land cover variables as features in the ensembles of decision trees used for classifying counties as either poor or not. We use the index “%IncMSE” (the percentage increase in the mean square error) to measure the relative importance of each predictor variable. This index is constructed by randomly assigning a value to a predictor variable; for a predictor that is relatively important there will be a larger rise in the MSE (in other words, a penalty) if an actual value is replaced with a random value, compared to the case of replacing values for other variables with random values. As shown in Figure 5, the BM and DMSP data showed more importance than the other two NTL variables in the RF model without environmental variables (panel a). In other words, even using a machine learning approach, there is no appearance of a gradient whereby the data from newer and finer resolution NTL sensors such as Luojia-01 provide better predictions of county poverty status. This lack of gradient is also apparent when environmental variables are included as predictors (panel b), and the inclusion of these variables also shows that the most important variables for predicting whether a county in rural China is classified as poor appear

to be the average elevation and temperature, rather than luminosity.

4.2 *Township-level Analysis*

The township-level results reported in Table 6 extend the analysis to finer administrative units, with a combined focus on the three household well-being indicators: per capita net income, poverty rates, and electrification. Recall that the median township in our sample covers just over 70 km², compared with 2200 km² for counties, so at this much finer scale the smaller pixel footprints of the third-generation sensors should, in principle, be especially advantageous. Yet the results mirror those at the county level, with no gradient of improvement across the sensors from the first to third generation. For example, in predicting net income per capita across all 265 townships, the adjusted R^2 values are very similar regardless of the sensor providing the NTL data, and using DMSP data gives predictions that are about as accurate as those coming from the newer Luojia-01. Likewise, for the poverty rate and electrification, predictive power remains modest and relatively flat across sensors. Thus, even where administrative units are small enough that sharper resolution and other improvements of third-generation sensors ought to come to the fore, predicting rural household activity and well-being does not seem to benefit from the improvements across the generations of sensors, possibly indicating that it is poorly suited to remote measurement from space. This motivates the next step of the analysis, which contrasts predictive power between sparsely populated and more densely populated areas.

The Table 6 results also show the heterogeneity that comes from variation in population density. Prior evidence for China shows more densely populated areas have closer relationships between VIIRS data (from both VNL and BM) and total GDP (this was at the county-level and included urban districts, the urban equivalent to counties in the administrative hierarchy), while the predictive accuracy of the DMSP data did not vary with respect to density, with this attributed to the DMSP top-coding issue in brightly-lit urban area (Zhang and Gibson, 2022). Elsewhere it has also been noted that relationships between NTL data and economic activity

indicators are far weaker in low density areas (Gibson, 2021; Gibson et al, 2021). To study this issue here, the township sample was split at median density (285 persons per km²); the low density townships (n=133) average 117 persons per km² and the high density ones (n=132) average 735 persons per km².

For each household well-being indicator and source of luminosity data in Table 6, there is far greater predictive power for high density townships compared to low density ones. For example, the equations for average per capita net household income—the indicator predicted best—have adjusted R^2 values of 0.47 in low-density townships and 0.62 in high-density ones, on average. The difference in predictability according to population density is even more stark for the poverty rate, with an average adjusted R^2 of 0.19 in low-density townships and 0.47 in high density ones. For the electrification rate, the corresponding averages are 0.12 and 0.43. In other words, the high-density townships have poverty (electrification) rates that are more than twice (thrice) as predictable as for the low-density townships when the predictor variables are all from remote sensing.

The patterns in Table 6 show predictive accuracy of remote measurement falls sharply with population sparsity: household well-being in low-density townships is less well predicted than in high-density ones, even if NTL data are combined with remotely sensed environmental and land-cover controls. This density effect also shows up in Table 2: county-level luminosity is about five times as responsive per square kilometre classified as urban built-up area as it is per the same area classified as village built-up land (3.8% vs 0.7%), consistent with the greater concentration of people and activities in denser, more urban settings. So even at the township scale (median area ~70 km²), the smaller pixel footprints, sensitivity to a wider range of lighting conditions and evening overpass of the third-generation sensors do not seem to overcome the fundamental constraint that the agricultural activities of dispersed rural households generate weak, spatially diffuse luminosity signals. The weaker predictions for low-density areas are

thus not likely to be a legacy of outdated sensors but instead reflects an inherent limit to remote measurement of dispersed rural household well-being. This raises a broader concern for the discussion that follows: if policy enthusiasm for satellite-based approaches runs ahead of their actual performance, the data poverty already facing low-density rural areas may deepen.

V. Discussion

Our analysis of 1,460 rural counties in China, together with 265 townships in a subset of those counties, used three generations of night-time lights sensors to test whether newer, more finely-grained and sensitive remote sensing systems improve the prediction of rural economic activity and household well-being. Across both scales, we do not find a gradient whereby more accurate predictions come from the newer sensors. This is despite the clear technical advances: modern systems have far smaller pixel footprints and better dim light sensitivity (and third generation systems have evening overpass times that are better aligned with household activity). Our ground-truthing showed that these third generation sensors can detect village-level built-up features more sharply than the earlier sensors, yet in statistical models of county and township outcomes the predictive gains fail to materialise.

The absence of improvement is especially striking at the township level. With a median area of just over 70 km²—thirty times smaller than counties—the township results should have been where the finer pixel footprints of third-generation sensors made the most difference.¹⁶ Instead, Table 6 shows that predictive accuracy for poverty rates remain modest and flat across sensor generations and while there were more accurate predictions of net per capita income at the township level, these predictions were just as good with the first generation sensors as with

¹⁶ In addition to a 30-fold difference in spatial scale, a further reason to expect advantages of third-generation sensors to show up at the township level compared to the county level is that key outcomes seem less spatially autocorrelated at township level: Moran's *I* for township average per capita net income is 0.04, versus 0.49 for county primary-sector GDP. Moran's *I* measures similarity with neighbours (values nearer 1 indicate stronger clustering; Anselin, 1988), so the more blurred DMSP data that may take on values from neighbours (Abrahams et al, 2018) get penalised less when the outcomes are spatially smooth. Hence township outcomes should have exposed a larger gain for finer sensors—yet Table 6 shows the gradient across generations is essentially flat.

data from the third generation ones. Extrapolating from this three-generation comparison, even further advances in sensor design may not yield substantially better predictions in low-density rural settings, given how flat the gradient already is. In other words, the payoffs to using newer and better NTL sensors to measure and predict rural outcomes appear to be fairly muted even as the literature reports gains from using these newer sensors for studying urban areas. In terms of the “horse race” posed in the Introduction: the problem is less with outdated sensors and is more the intrinsic unsuitability of rural household activity for remote measurement from space.

Taken together, these findings point to a structural constraint rather than a sensor limitation. Agriculture, the predominant rural activity, generates little concentrated night-time illumination, and dispersed households produce signals too weak and diffuse for satellites to capture reliably. This conclusion is consistent with earlier studies showing that night-time lights are a poor proxy for economic activity and well-being in rural contexts—whether in rural areas of China and Indonesia (Gibson et al., 2021; Zhang and Gibson, 2022), in cross-country settings where agriculture and forestry account for large GDP shares (Keola et al., 2015), or in multi-country analyses highlighting very low elasticities of lights with respect to agricultural GDP (Bluhm and McCord, 2022). Our results extend that conclusion with more comprehensive coverage and finer spatial detail: even at the township scale, predictive accuracy does not seem to improve with newer sensors. The implication is that investing in more finely grained remote measurement systems may help urban analysis while not bringing much benefit for measuring rural household well-being.

Some support for our central finding, of a flat gradient across sensor generations for the prediction equations, comes from a recent review of 60 poverty prediction studies using satellite imagery, which found no systematic link between spatial resolution of the imagery and subsequent prediction accuracy (Hall et al., 2023). On the other hand, a possible criticism is that influential recent work has shifted towards daytime imagery and machine learning rather

than night-time lights alone, so our results could appear tangential. Yet luminosity remains a core element of the poverty-from-space toolkit: some studies in economics directly proxy for poverty using NTL data, including Smith and Wills (2018) and Maldonado (2023), while in a related dimension of welfare Zhang et al (2023) review over two dozen recent papers that rely on NTL data to study inequality. Moreover, NTL are still widely applied in China at the county and township level, using DMSP, VIIRS, or LuoJia-01 data to study poverty patterns (e.g. Xu et al, 2021; Lin et al, 2022). Even in approaches that combine daytime imagery with machine learning, NTL is often retained as a key feature. Our own models already integrate NTL with other remotely sensed covariates—land cover and environmental factors—yet the predictive accuracy remained modest with no sign of improved predictions across sensor generations. These results show that our findings are directly relevant to the wider literature: the constraints we document in low-density rural areas are structural, not simply a reflection of prior studies using outdated sensors or limited imagery inputs.

VI. Conclusions: Implications for Measurement

In arguing that newer may not be better, in terms of the types of data used to study household well-being in data-poor environments, we are not defending the status quo. Rural livelihoods will remain spatially correlated, given dependence on environmental inputs. Rural samples will therefore be less informative than samples of the same size in less correlated settings. Even so, there is scope to improve surveys. Influential past experiments—such as Beegle et al (2012), and the broader set reviewed by De Weerd et al (2020)—contributed to innovations in survey practice for studying household well-being in developing countries. Future experiments could again advance measurement. For example, samples are traditionally highly clustered, with a dozen or more households per enumeration area (EA). Less clustered designs are now feasible under FAO and World Bank (2018) guidelines for 7-day recall food modules instead of the traditional diary surveys that kept interview teams in each EA for many days (and once there

surveying more households was easier than going to a new village).¹⁷ With one-and-done recall surveys, going to fewer households per EA but to more EAs overall could be both feasible and more informative.^{18,19}

Interest in such experiments may, however, be limited by the apparent success of remote measurement studies using satellite imagery to monitor household well-being. Donors may reason that surveys are less necessary if satellites can substitute. Our results suggest caution. Rural economic activity and household well-being appear poorly suited to remote measurement. The limitations seem most severe in low-density areas. Ironically, these are also the most costly places to survey: travel within an EA takes longer, neighbouring EAs are harder to combine in a single workload, and the listing stage prior to the final selection of households to interview can take a day or more in sparsely settled villages.²⁰ Thus, the places where satellite-detected data seems to add least are often those where survey costs are highest. This makes the case for renewed innovation in surveys to measure well-being in these data-poor environments rather than in replacement of surveys with satellite data.

A more constructive approach is to view satellites and surveys as complements rather than substitutes. For example, surveys and censuses can be combined with remote sensing data to improve poverty maps (e.g., van der Weide et al, 2024). Satellite-derived gridded population estimates, such as WorldPop that rely on NTL data, can provide sampling frames where

¹⁷ At minimum, interviewers for diary surveys return each week to pick up the completed diary and distribute a new diary for the coming week but with illiterate households interviewers often need to revisit every second day (Beegle et al, 2012).

¹⁸ The potential time savings are apparent from a recent experiment where interviewers alternated between diary and recall formats: they had ample free time with recall surveys but struggled to complete workloads with diaries (Sharp et al., 2022).

¹⁹ Many SDGs are tail-based measures, such as proportions of the population either hungry or poor, and so they depend not only on measures of means and totals (what many household economic surveys historically focused on) but also on variances (Gibson, 2020). Hence, sample efficiency matters to SDG monitoring.

²⁰ The DHS *Sampling and Household Listing Manual* notes that mapping and listing often occupies a full field day per EA (and up to two days in sparsely populated areas):

<https://www.dhsprogram.com/publications/publication-dhsm4-dhs-questionnaires-and-manuals.cfm> Listing is also needed to update sampling weights because the population basis on which an EA was selected (e.g. a prior census enumeration) is typically out of date by the time of the survey.

censuses are missing or outdated (Thomson et al., 2020). Earth-observation data can also reduce survey costs directly, for instance by helping to pre-identify dwellings and streamline the listing stage. Coupled with the opportunities from shorter recall periods and more lightly clustered designs, such integration could make future surveys both cheaper and more informative. Realising this potential requires not abandoning surveys, but sustaining a balanced research agenda where the investments in remote measurement approaches complement, rather than crowd out, the next generation of survey experiments.

References

- Abrahams, A., Oram, C., & Lozano-Gracia, N. (2018). Deblurring DMSP nighttime lights: A new method using Gaussian filters and frequencies of illumination. *Remote Sensing of Environment*, 210, 242-258.
- Angrist, N., Goldberg, P. K., & Jolliffe, D. (2021). Why is growth in developing countries so hard to measure? *Journal of Economic Perspectives*, 35(3), 215-42.
- Anselin, L. (1988). *Spatial Econometrics: Methods and Models*, Dordrecht: Kluwer Academic Publishers.
- Asher, S., Lunt, T., Matsuura, R., & Novosad, P. (2021). Development research at high geographic resolution: an analysis of night-lights, firms, and poverty in India using the SHRUG open data platform. *The World Bank Economic Review*, 35(4), 845-871.
- Beegle, K., De Weerd, J., Friedman, J., & Gibson, J. (2012). Methods of household consumption measurement through surveys: Experimental results from Tanzania. *Journal of Development Economics*, 98(1), 3-18.
- Bluhm, R., & Krause, K. (2022). Top lights: Bright cities and their contribution to economic development. *Journal of Development Economics*, 157(1), 102880.
- Bluhm, R., & McCord, G. (2022). What can we learn from nighttime lights for small geographies? Measurement errors and heterogeneous elasticities. *Remote Sensing*, 14(5), 1190.
- Breiman, L. (2001). Random forests. *Machine Learning*, 45(1), 5-32.
- Bruederle, A., & Hodler, R. (2018). Nighttime lights as a proxy for human development at the local level. *PloS one*, 13(9), e0202231.
- Burke, M., Driscoll, A., Lobell, D., & Ermon, S. (2022). Using satellite imagery to understand and promote sustainable development. *HAI Policy Brief*, Stanford Institute for Human-Centered Artificial Intelligence. <https://hai.stanford.edu/policy-brief-using-satellite-imagery-understand-and-promote-sustainable-development>
- Chen, Y. (2025). Geographically heterogeneous spatial inequality in the People's Republic of China: A luminosity-based analysis of prefectural cities and counties. *Asian Development Review*, 42(2), 55-81.
- Chen, Z., Luo, H., Li, M., Lin, J., Zhang, X., & Li, S. (2025). Fine-scale poverty estimation by integrating SDGSAT-1 glimmer images and urban functional zoning data. *Remote Sensing of Environment*, 329, 114925.
- Chen, X., & Nordhaus, W. (2011). Using luminosity data as a proxy for economic statistics. *Proceedings of the National Academy of Sciences*, 108(21), 8589-8594.
- Chen, X., & Nordhaus, W. (2015). A test of the new VIIRS lights data set: Population and economic output in Africa. *Remote Sensing*, 7(4), 4937-4947.
- Castelló-Climent, A., Chaudhary, L., & Mukhopadhyay, A. (2018). Higher education and prosperity: From Catholic missionaries to luminosity in India. *The Economic Journal*, 128(616), 3039-3075.
- Dai, Z., Hu, Y., & Zhao, G. (2017). The suitability of different nighttime light data for GDP estimation at different spatial scales and regional levels. *Sustainability*, 9(2), 305.

- Dang, H. A., Carletto, C., & Jolliffe, D. (2025). Better tracking SDG progress with fewer resources? A call for more innovative data uses. *World Development Perspectives*, 39, 100721.
- De Weerd, J., Gibson, J., & Beegle, K. (2020). What can we learn from experimenting with survey methods? *Annual Review of Resource Economics*, 12, 431-447.
- Dong, B., Zhang, R., Li, S., Ye, Y., & Huang, C. (2025). A meta-analysis for the nighttime light remote sensing data applied in urban research: Key topics, hotspot study areas and new trends. *Science of Remote Sensing*, 11, 100186.
- Elbers, C., Lanjouw, J., & Lanjouw, P. (2003). Micro-level estimation of poverty and inequality. *Econometrica*, 71(1), 355-364.
- Elvidge, C., Baugh, K., Zhizhin, M., & Hsu, F-C. (2013). Why VIIRS data are superior to DMSP for mapping nighttime lights. *Proceedings of the Asia-Pacific Advanced Network*, 35(0), 62.
- Elvidge, C., Zhizhin, M., Ghosh, T., Hsu, F-C., & Taneja, J. (2021). Annual time series of global VIIRS nighttime lights derived from monthly averages: 2012 to 2019. *Remote Sensing*, 13(5), 922.
- Fenz, K., Mitterling, T., Martinez, A., Bulan, J., Durante, R., Martillan, M., Addawe, M., & Roitner-Fransecky, I. (2024). Compiling granular population data using geospatial information. *Asian Development Review*, 41(1), 1-39.
- Food and Agriculture Organization of the United Nations (FAO) and the World Bank. (2018). *Food Data Collection in Household Consumption and Expenditure Surveys: Guidelines for Low-and Middle-Income Countries*. Accessed on 25 August, 2025 from: <https://openknowledge.worldbank.org/handle/10986/32503> Rome & Washington D.C.: Food and Agriculture Organization (FAO) and the World Bank.
- Ghosh, T., Baugh, K., Elvidge, C., Zhizhin, M., Poyda, A., & Hsu, F-C. (2021). Extending the DMSP nighttime lights time series beyond 2013. *Remote Sensing*, 13(24), 5004.
- Gibson, J. (2019). Are you estimating the right thing? An editor reflects. *Applied Economic Perspectives and Policy*, 41(3), 329-350.
- Gibson, J. (2020). Measuring chronic hunger from diet snapshots. *Economic Development and Cultural Change*, 68(3), 813-838.
- Gibson, J. (2021). Better night lights data, for longer. *Oxford Bulletin of Economics and Statistics*, 83(3), 770-791.
- Gibson, J., & Boe-Gibson, G. (2021). Nighttime lights and county-level economic activity in the United States: 2001 to 2019. *Remote Sensing*, 13(14), 2741.
- Gibson, J., Datt, G., Murgai, R., & Ravallion, M. (2017). For India's rural poor, growing towns matter more than growing cities. *World Development*, 98, 413-429.
- Gibson, J., Jiang, Y., & Susantono, B. (2023). Revisiting the role of secondary towns: How different types of urban growth relate to poverty in Indonesia. *World Development*, 169, 106281.
- Gibson, J., Kim, B., & Olivia, S. (2011). Spatial correlation in household choices in rural Indonesia. *Asian Economic Journal*, 25(3), 271-289.

- Gibson, J., Olivia, S., & Boe-Gibson, G. (2020). Night lights in economics: Sources and uses. *Journal of Economic Surveys*, 34(5), 955-980.
- Gibson, J., Olivia, S., Boe-Gibson, G., & Li, C. (2021). Which night lights data should we use in economics, and where? *Journal of Development Economics*, 149, 102602.
- Gibson, J., Alimi, O., & Boe-Gibson, G. (2025). Lost in translation? A critical review of economics research using nighttime lights data. *Remote Sensing*, 17(7), 1130.
- Goldblatt, R., Heilmann, K., & Vaizman, Y. (2020). Can medium-resolution satellite imagery measure economic activity at small geographies? Evidence from Landsat in Vietnam. *The World Bank Economic Review*, 34(3), 635-653.
- Grömping, U. (2015). Variable importance in regression models. *Wiley Interdisciplinary Reviews: Computational Statistics*, 7, 137-152.
- Hall, O., Dompae, F., Wahab, I., & Dzanku, F. M. (2023). A review of machine learning and satellite imagery for poverty prediction: Implications for development research and applications. *Journal of International Development*, 35(7), 1753-1768.
- Henderson, V., Storeygard, A., & Weil, D. (2012). Measuring economic growth from outer space. *American Economic Review*, 102(2), 994-1028.
- Jean, N., Burke, M., Xie, M., Davis, W., Lobell, D., & Ermon, S. (2016). Combining satellite imagery and machine learning to predict poverty. *Science*, 353(6301), 790-794.
- Jerven, M., & Johnston, D. (2015). Statistical tragedy in Africa? Evaluating the data base for African economic development. *The Journal of Development Studies*, 51(2), 111-115.
- Jiang, W., Liu, J., Long, T., Liu, M., Pang, Z., Luo, G., ... & Wang, L. (2025). Preliminary analysis of factors affecting economic well-being based on SDGSAT-1 nighttime light remote sensing and household survey data. *ISPRS Annals of the Photogrammetry, Remote Sensing and Spatial Information Sciences*, 421-426.
- Jing, X., Shao, X., Cao, C., Fu, X., & Yan, L. (2015). Comparison between the Suomi-NPP Day-Night Band and DMSP-OLS for correlating socio-economic variables at the provincial level in China. *Remote Sensing*, 8(1), 17.
- Keola, S., Andersson, M., & Hall, O. (2015). Monitoring economic development from space: using nighttime light and land cover data to measure economic growth. *World Development*, 66, 322-334.
- Khachiyani, A., Thomas, A., Zhou, H., Hanson, G., Cloninger, A., Rosing, T., & Khandelwal, A. (2022). Using neural networks to predict micro-spatial economic growth. *American Economic Review: Insights*, 4(4), 491-506.
- Kim, B., Gibson, J., & Boe-Gibson, G. (2024). Measurement errors in popular night lights data may bias estimated impacts of economic sanctions: Evidence from closing the Kaesong Industrial Zone. *Economic Inquiry*, 62(1), 375-389.
- Li, C., Chen, F., Wang, N., Yu, B., & Wang, L. (2023). SDGSAT-1 nighttime light data improve village-scale built-up delineation. *Remote Sensing of Environment*, 297, 113764.
- Li, X., Liu, Z., Chen, X., & Sun, J. (2019). Assessing the ability of LuoJia 1-01 imagery to detect feeble nighttime lights. *Sensors*, 19(17), 3708.

- Lin, J., Luo, S., & Huang, Y. (2022). Poverty estimation at the county level by combining LuoJia1-01 nighttime light data and points of interest. *Geocarto International*, 37(12), 3590-3606.
- Liu, H., Luo, N., & Hu, C. (2020). Detection of county economic development using LJ1-01 nighttime light imagery: A comparison with NPP-VIIRS data. *Sensors*, 20(22), 6633.
- Lobell, D., Azzari, G., Burke, M., Gurlay, S., Jin, Z., Kilic, T., & Murray, S. (2020). Eyes in the sky, boots on the ground: Assessing satellite-and ground-based approaches to crop yield measurement and analysis. *American Journal of Agricultural Economics*, 102(1), 202-219.
- Maldonado, L. (2023). Living in darkness: rural poverty in Venezuela. *Journal of Applied Economics*, 26(1), 2168464.
- Nechaev, D., Zhizhin, M., Poyda, A., Ghosh, T., Hsu, F. C., & Elvidge, C. (2021). Cross-sensor nighttime lights image calibration for DMSP/OLS and SNPP/VIIRS with residual U-net. *Remote Sensing*, 13(24), 5026.
- Nordhaus, W., & Chen, X. (2015). A sharper image? Estimates of the precision of nighttime lights as a proxy for economic statistics. *Journal of Economic Geography*, 15(1), 217-246.
- Olivia, S., Gibson, J., Rozelle, S., Huang, J., & Deng, X. (2011). Mapping poverty in rural China: how much does the environment matter? *Environment and Development Economics*, 16(2), 129-153.
- Park, A., Wang, S., & Wu, G. (2002). Regional poverty targeting in China. *Journal of Public Economics*, 86(1), 123-153.
- Puttanapong, N., Prasertsoong, N., & Peechapat, W. (2023). Predicting provincial Gross Domestic Product using satellite data and machine learning methods: A case study of Thailand. *Asian Development Review*, 40(2), 39-85.
- Rogers, G., Koper, P., Ruktanonchai, C., Ruktanonchai, N., Utazi, E., Woods, D., ... & Sorichetta, A. (2023). Exploring the relationship between temporal fluctuations in satellite nighttime imagery and human mobility across Africa. *Remote Sensing*, 15(17), 4252.
- Román, M., Wang, Z., Sun, Q., Kalb, V., Miller, S., Molthan, A., Schultz, L., Bell, J., Stokes, E., Pandey, B., & Seto, K. (2018). NASA's Black Marble nighttime lights product suite. *Remote Sensing of the Environment*, 210, 113-43.
- Sharp, M. K., Buffière, B., Himelein, K., Troubat, N., & Gibson, J. (2022). Effects of data collection methods on estimated household consumption and survey costs. *Policy Research Working Paper No. 10029*, The World Bank.
- Shi, K., Yu, B., Huang, Y., Hu, Y., Yin, B., Chen, Z., Chen, L., & Wu, J. (2014). Evaluating the ability of NPP-VIIRS nighttime light data to estimate the gross domestic product and the electric power consumption of China at multiple scales: A comparison with DMSP-OLS data. *Remote Sensing*, 6(2), 1705-1724.
- Smith, B., & Wills, S. (2018). Left in the dark? Oil and rural poverty. *Journal of the Association of Environmental and Resource Economists*, 5(4), 865-904.

- Song, W., & Deng, X. (2017). Land-use/land-cover change and ecosystem service provision in China. *Science of the Total Environment*, 576, 705-719.
- Thomson, D. R., Rhoda, D. A., Tatem, A. J., & Castro, M. C. (2020). Gridded population survey sampling: a systematic scoping review of the field and strategic research agenda. *International Journal of Health Geographics*, 19(1), 34.
- Tuttle, B., Anderson, S., Sutton, P., Elvidge, C., & Baugh, K. (2013). It used to be dark here. *Photogrammetric Engineering & Remote Sensing*, 79(3), 287-297.
- Van Der Weide, R., Blankespoor, B., Elbers, C., & Lanjouw, P. (2024). How accurate is a poverty map based on remote sensing data? An application to Malawi. *Journal of Development Economics*, 171, 103352.
- Watmough, G., Marcinko, C., Sullivan, C., Tschirhart, K., Mutuo, P., Palm, C., & Svenning, J. (2019). Socio-ecologically informed use of remote sensing data to predict rural household poverty. *Proceedings of the National Academy of Sciences*, 116(4), 1213-1218.
- Wu, J., Zhang, Z., Yang, X., & Li, X. (2021). Analyzing pixel-level relationships between LuoJia 1-01 nighttime light and urban surface features by separating the pixel blooming effect. *Remote Sensing*, 13(23), 4838.
- Xie, Q., Cai, C., Jiang, Y., Zhang, H., Wu, Z., & Xu, J. (2024). Investigating the performance of SDGSAT-1/GIU and NPP/VIIRS nighttime light data in representing nighttime vitality and its relationship with the built environment: A comparative study in Shanghai, China. *Ecological Indicators*, 160, 111945.
- Xu, J., Song, J., Li, B., Liu, D., & Cao, X. (2021). Combining night time lights in prediction of poverty incidence at the county level. *Applied Geography*, 135, 102552.
- Yeh, C., Perez, A., Driscoll, A., Azzari, G., Tang, Z., Lobell, D., Ermon, S., & Burke, M. (2020). Using publicly available satellite imagery and deep learning to understand economic well-being in Africa. *Nature Communications*, 11(1), 2583.
- Zhang, G., Guo, X., Li, D., & Jiang, B. (2019). Evaluating the potential of LJ1-01 nighttime light data for modelling socio-economic parameters. *Sensors*, 19(6), 1465.
- Zhang, X., & Gibson, J. (2022). Using multi-source nighttime lights data to proxy for county-level economic activity in China from 2012 to 2019. *Remote Sensing*, 14(5), 1282.
- Zhang, X., Gibson, J., & Deng, X. (2023). Remotely too equal: Popular DMSP night-time lights data understate spatial inequality. *Regional Science Policy & Practice*, 15(9), 2106-2126.
- Zhang, L., Xie, L., & Zheng, X. (2023). Across a few prohibitive miles: The impact of the Anti-Poverty Relocation Program in China. *Journal of Development Economics*, 160, 102945.

Table 1. Attributes of the various NTL data sources and data products

	DMSF	VNL	Black Marble	LuoJia-01	SDGSAT-1
<i>Satellite/Sensor Attributes</i>					
Operator	US DoD	NASA/NOAA		Wuhan University	CBAS
Sensor	OLS	VIIRS		CMOS	TIS, MII, GIU
Available years	1992-2019	2012-present		June 2018- March 2019	November 2021-present
Wavelength range	500-900 nm	500-900 nm		460-980 nm	P: 444-910 nm, B: 424-526 nm, G: 506-612 nm
Orbit type and height	Polar, 850 km	Polar, 827 km		Polar, 645 km	Sun-synchronous orbit, 505 km
Pixel footprint at nadir	25 km ²	0.55 km ²		0.02 km ²	0.0001 km ² (Panchromatic band)
Swath	3000 km	3000 km		250 km	300 km
Revisit time	12 hr	12 hr		3-5 days	11 days
Pixel saturation	Saturated	Not saturated		Not saturated	Not saturated
On-board calibration	No	Yes		Yes	Yes
<i>Data Products</i>					
Creator of annual composites	EOG	EOG	NASA	Wuhan University	CBAS
Tiled	No	No	Yes, 648 tiles	Yes	Yes
Quantization	6-bit (n=64)	14 bit (n=16,384)	16 bit (n=65,536)	14 bit (n=16,384)	16 bit (n=65,536)
Masking of ephemeral light sources	No	Yes	Yes	Yes	Yes
Stray-light correction	No	Yes, from 2014	Yes	Yes	Yes
User choice over angle of detection	No	No	Yes	No	No
Treatment of snow	No	No	Yes	No	No

Note: DoD is Department of Defense, OLS is Operational Linescan System, VIIRS is Visible Infrared Imaging Radiometer Suite, EOG is Earth Observation Group, CBAS is the International Research Center of Big Data for Sustainable Development Goals. P is panchromatic band, B, G, R is Blue, Green, and Red respectively. TIS is the Thermal Infrared Spectrometer, MII is Multispectral Imager for Inshore, GIU is Glimmer Imager for Urbanization. Satellite/sensor attributes for VNL and Black Marble are the same, so they share the same column (but attributes of these data products differ).

Table 2: Relationships between Landsat detected built-up area and luminosity (sum of lights)

	(1)	(2)	(3)	(4)
----- DMSP -----				
Urban (towns and cities)	0.045*** (0.004)			0.028*** (0.002)
Village residential area		0.008*** (0.000)		0.004*** (0.000)
Industrial/infrastructural			0.019*** (0.004)	0.015*** (0.001)
Adjusted R²	0.303	0.256	0.105	0.416
----- VNL -----				
Urban (towns and cities)	0.037*** (0.003)			0.021*** (0.003)
Village residential area		0.007*** (0.000)		0.004*** (0.000)
Industrial/infrastructural			0.015*** (0.003)	0.013*** (0.003)
Adjusted R²	0.274	0.251	0.100	0.391
----- Black Marble -----				
Urban (towns and cities)	0.041*** (0.004)			0.030*** (0.004)
Village residential area		0.006*** (0.000)		0.003*** (0.000)
Industrial/infrastructural			0.018*** (0.004)	0.015*** (0.003)
Adjusted R²	0.276	0.177	0.114	0.366
----- Luojia-01 -----				
Urban (towns and cities)	0.028*** (0.002)			0.019*** (0.002)
Village residential area		0.005*** (0.000)		0.002*** (0.000)
Industrial/infrastructural			0.013*** (0.003)	0.011*** (0.002)
Adjusted R²	0.194	0.134	0.088	0.269

Notes: The dependent variable is county-level luminosity. Intercepts are not reported to save space. Built-up area is measured in km² and the sum of lights in logs, so coefficients are (approximately) percentage differences in luminosity per 1 km² of each type of built up area. The land use for industrial and infrastructural land includes factories, mines and quarries, airports and roads. Based on $n=1460$ counties, with robust standard errors in () and ***, **, and * denoting statistical significance at 1%, 5% and 10%.

Table 3: The predictive power of night-time lights data for county-level primary sector GDP in rural areas of China

	No control variables			Controls for land cover and environmental factors		
	ln (sum of lights)	ln (lights per km ²)	% of pixels illuminated	ln (sum of lights)	ln (lights per km ²)	% of pixels illuminated
DMSP	0.612*** (0.021)	0.559*** (0.022)	0.571*** (0.022)	0.226*** (0.023)	0.084*** (0.024)	0.080*** (0.025)
Adjusted R²	0.374	0.313	0.325	0.705	0.688	0.688
VIIRS Night Lights	0.648*** (0.020)	0.569*** (0.022)	0.527*** (0.022)	0.283*** (0.021)	0.122*** (0.024)	0.036 (0.025)
Adjusted R²	0.420	0.323	0.277	0.721	0.691	0.686
Black Marble, weighted average	0.628*** (0.020)	0.560*** (0.022)	0.410*** (0.024)	0.210*** (0.022)	0.083*** (0.025)	0.011 (0.023)
Adjusted R²	0.394	0.314	0.168	0.704	0.688	0.685
Luojia-01	0.359*** (0.024)	0.440*** (0.024)	0.279*** (0.025)	0.107*** (0.017)	0.028*** (0.020)	0.031* (0.017)
Adjusted R²	0.128	0.193	0.077	0.694	0.686	0.686

Notes: The dependent variable is the logarithm of primary sector GDP. Coefficients are for standardized variables to aid comparability across outcomes and specifications of NTL data. The sample is $n=1460$ rural counties. Robust standard errors in (), ***, **, and * denote statistical significance at 1%, 5% and 10% levels. The control variables in columns (4) to (6) are elevation, precipitation, temperature, and five types of land cover (urban, village, industrial and infrastructural, cultivated land and forest).

Table 4: The predictive power of night-time lights data for county-level poverty status in rural areas of China

	No control variables			Controls for land cover and environmental factors		
	ln (sum of lights)	ln (lights per km ²)	% of pixels illuminated	ln (sum of lights)	ln (lights per km ²)	% of pixels illuminated
DMSP	-0.355*** (0.024)	-0.371*** (0.024)	-0.356*** (0.024)	-0.186*** (0.038)	-0.169*** (0.039)	-0.146*** (0.040)
Adjusted R²	0.126	0.137	0.126	0.192	0.189	0.185
VIIRS Night Lights	-0.342*** (0.025)	-0.360*** (0.024)	-0.345*** (0.025)	-0.165*** (0.036)	-0.158*** (0.038)	-0.111*** (0.040)
Adjusted R²	0.117	0.129	0.119	0.190	0.187	0.182
Black Marble, weighted average	-0.357*** (0.024)	-0.367*** (0.024)	-0.343*** (0.025)	-0.159*** (0.036)	-0.164*** (0.040)	-0.146*** (0.036)
Adjusted R²	0.127	0.134	0.117	0.189	0.188	0.187
Luojia-01	-0.255*** (0.025)	-0.346*** (0.025)	-0.205*** (0.025)	-0.136*** (0.028)	-0.155*** (0.032)	-0.143*** (0.028)
Adjusted R²	0.064	0.120	0.093	0.191	0.191	0.193

Notes: The dependent variable indicates the poverty status of each county. Coefficients are for standardized variables to aid comparability across outcomes and specifications of NTL data. The sample is $n=1460$ rural counties. Robust standard errors in (), ***, **, and * denote statistical significance at 1%, 5% and 10% levels. The control variables in columns (4) to (6) are elevation, precipitation, temperature, and five types of land cover (urban, village, industrial and infrastructural, cultivated land and forest).

Table 5: The predictive power of night-time lights data for county fiscal revenue in rural areas of China

	No control variables			Controls for land cover and environmental factors		
	ln (sum of lights)	ln (lights per km ²)	% of pixels illuminated	ln (sum of lights)	ln (lights per km ²)	% of pixels illuminated
DMSP	0.636*** (0.021)	0.618*** (0.021)	0.606*** (0.021)	0.451*** (0.026)	0.338*** (0.028)	0.313*** (0.029)
Adjusted R²	0.397	0.378	0.361	0.614	0.580	0.569
VIIRS Night Lights	0.668*** (0.020)	0.629*** (0.020)	0.601*** (0.021)	0.478*** (0.024)	0.365*** (0.027)	0.339*** (0.029)
Adjusted R²	0.443	0.393	0.360	0.635	0.586	0.576
Black Marble, weighted average	0.711*** (0.019)	0.658*** (0.020)	0.517*** (0.023)	0.489*** (0.024)	0.396*** (0.028)	0.227*** (0.027)
Adjusted R²	0.502	0.430	0.266	0.634	0.591	0.557
Luojia-01	0.437*** (0.024)	0.548*** (0.022)	0.390*** (0.024)	0.211*** (0.020)	0.208*** (0.024)	0.131*** (0.021)
Adjusted R²	0.190	0.300	0.152	0.567	0.559	0.547

Notes: The dependent variable is the logarithm of fiscal revenue. Coefficients are for standardized variables to aid comparability across outcomes and specifications of NTL data. The sample is $n=1460$ rural counties. Robust standard errors in (), ***, **, and * denote statistical significance at 1%, 5% and 10% levels. The control variables in columns (4) to (6) are elevation, precipitation, temperature, and five types of land cover (urban, village, industrial and infrastructural, cultivated land and forest).

Table 6: Predictive power of night-time lights data for township-level indicators of household well-being (all specifications use the township sum-of-lights and control for land cover and environmental factors)

	Average per capita net household income			Poverty rate			Electrification rate of dwellings		
	All townships	Low density	High density	All townships	Low density	High density	All townships	Low density	High density
DMSP	0.079*	0.103	0.157**	-0.096**	-0.094	-0.252**	0.151**	0.095	0.014
	(0.049)	(0.073)	(0.068)	(0.048)	(0.065)	(0.119)	(0.070)	(0.076)	(0.022)
Adjusted R²	0.568	0.469	0.623	0.595	0.199	0.481	0.121	0.110	0.431
VNL	0.119**	0.163*	0.120*	-0.063	-0.085	-0.042	0.209***	0.154*	0.003
	(0.052)	(0.086)	(0.070)	(0.051)	(0.077)	(0.124)	(0.074)	(0.090)	(0.023)
Adjusted R²	0.572	0.476	0.616	0.591	0.193	0.463	0.132	0.120	0.429
Black Marble	0.127**	0.172**	0.128*	-0.090*	-0.101	-0.241*	0.229***	0.155*	0.001
	(0.052)	(0.088)	(0.077)	(0.050)	(0.079)	(0.135)	(0.073)	(0.092)	(0.025)
Adjusted R²	0.573	0.477	0.615	0.593	0.196	0.476	0.138	0.120	0.429
Luojia-01	0.093*	0.090	0.098**	-0.021	-0.050	-0.090	0.170**	0.142	0.011
	(0.048)	(0.100)	(0.042)	(0.047)	(0.090)	(0.074)	(0.068)	(0.104)	(0.014)
Adjusted R²	0.570	0.464	0.623	0.589	0.187	0.468	0.126	0.113	0.432

Notes: Coefficients are for standardized variables to aid comparability across outcomes. The sample is split amongst 265 townships into the above median (n=132) and below median (n=133) population density sub-samples. Robust standard errors in (), ***, **, and * denote statistical significance at 1%, 5% and 10% levels. The controls for land cover and environmental factors are those noted in Tables 3-5.

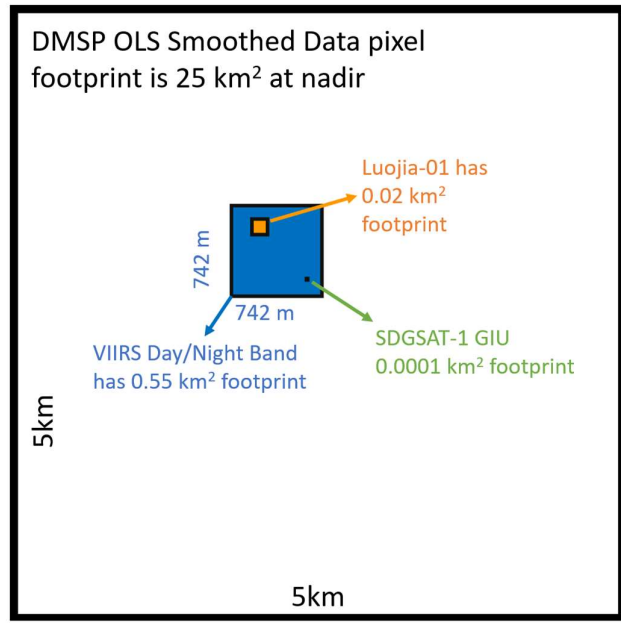


Figure 1. Comparison of the pixel footprints, at nadir, for three generations of NTL sensors (After: Elvidge et al (2013) “Why VIIRS data are superior to DMSP for mapping night time lights”).

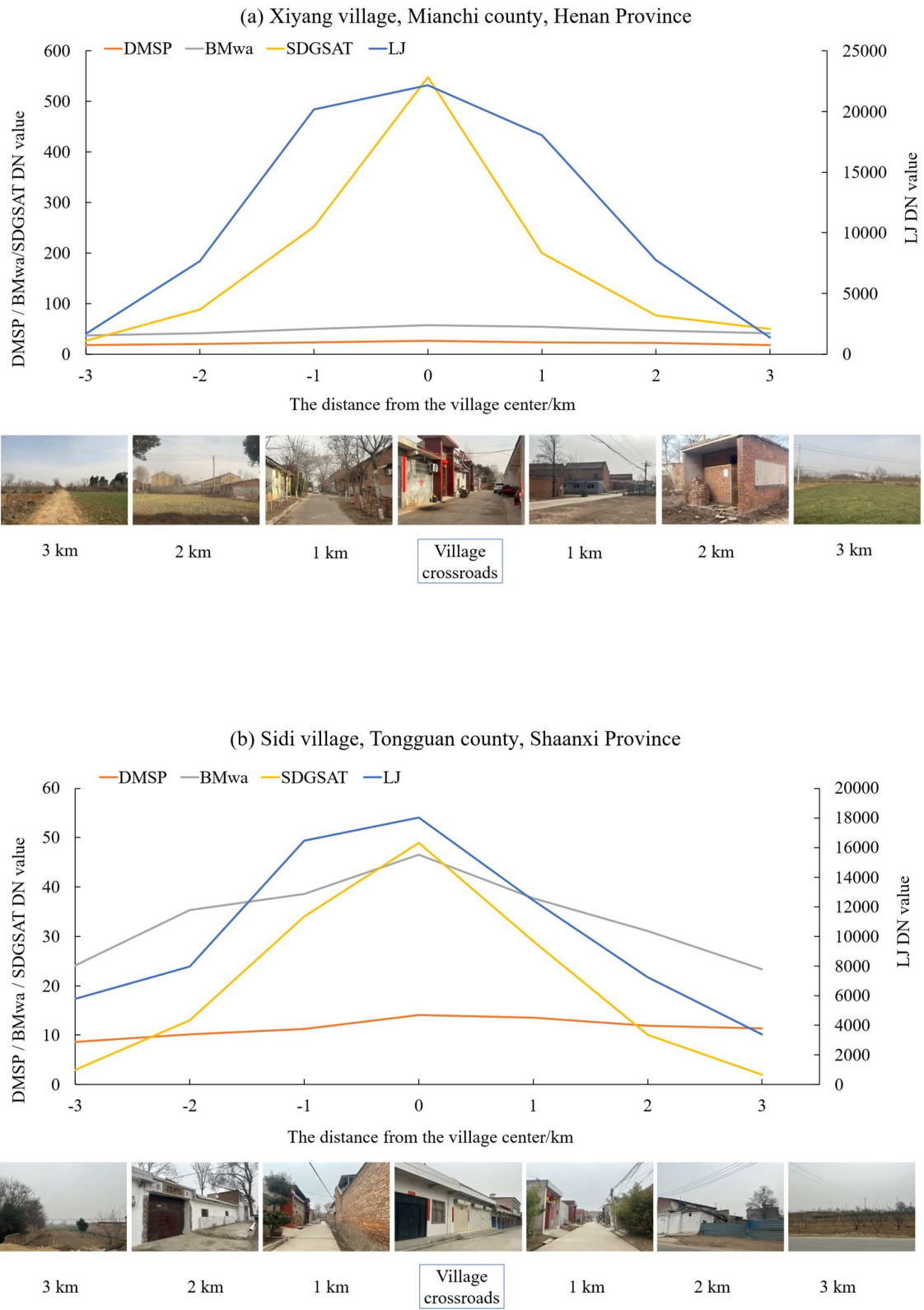


Figure 2: Illustrating spatial resolution and sensitivity with village ground-truthing transects

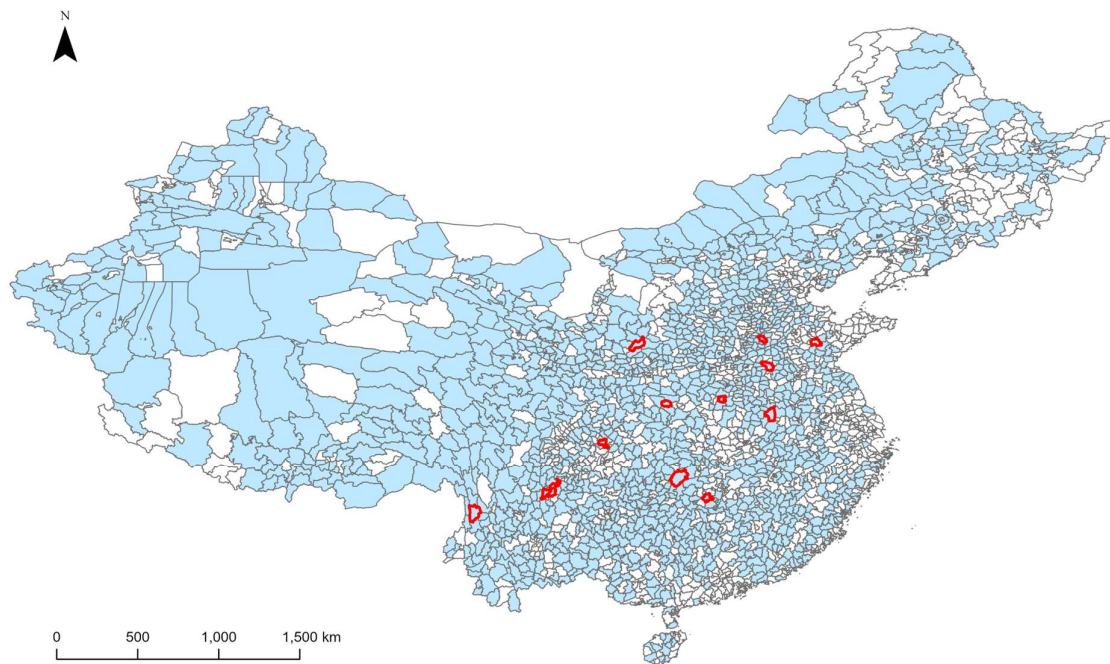


Figure 3: Location map for the $n=1460$ rural counties
(counties with red borders have household-level census data used to calculate township indicators)

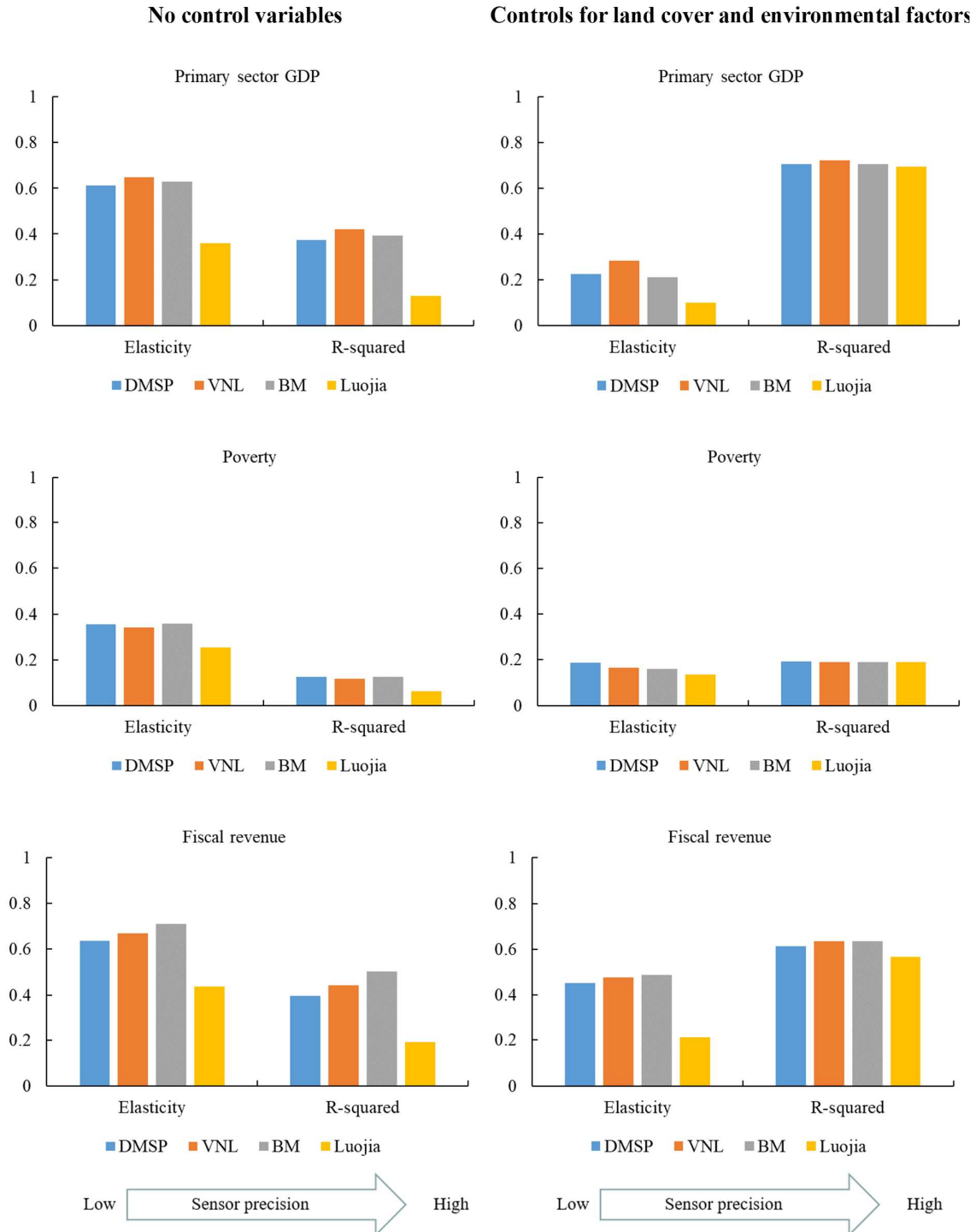
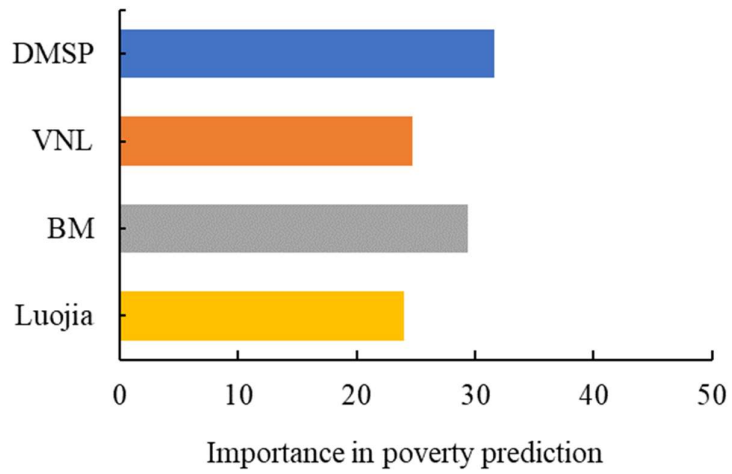


Figure 4: Variation in the Predictive Performance of NTL data from Sensors of Varying Precision
 Notes: Based on $n=1460$ counties, with full results reported in Tables 3-5. The sign of the elasticities of poverty with respect to luminosity are reversed for display purposes. The luminosity indicator used is the sum of lights. The R-squared reported is the adjusted R-squared to account for the different number of covariates.

(a)



(b)

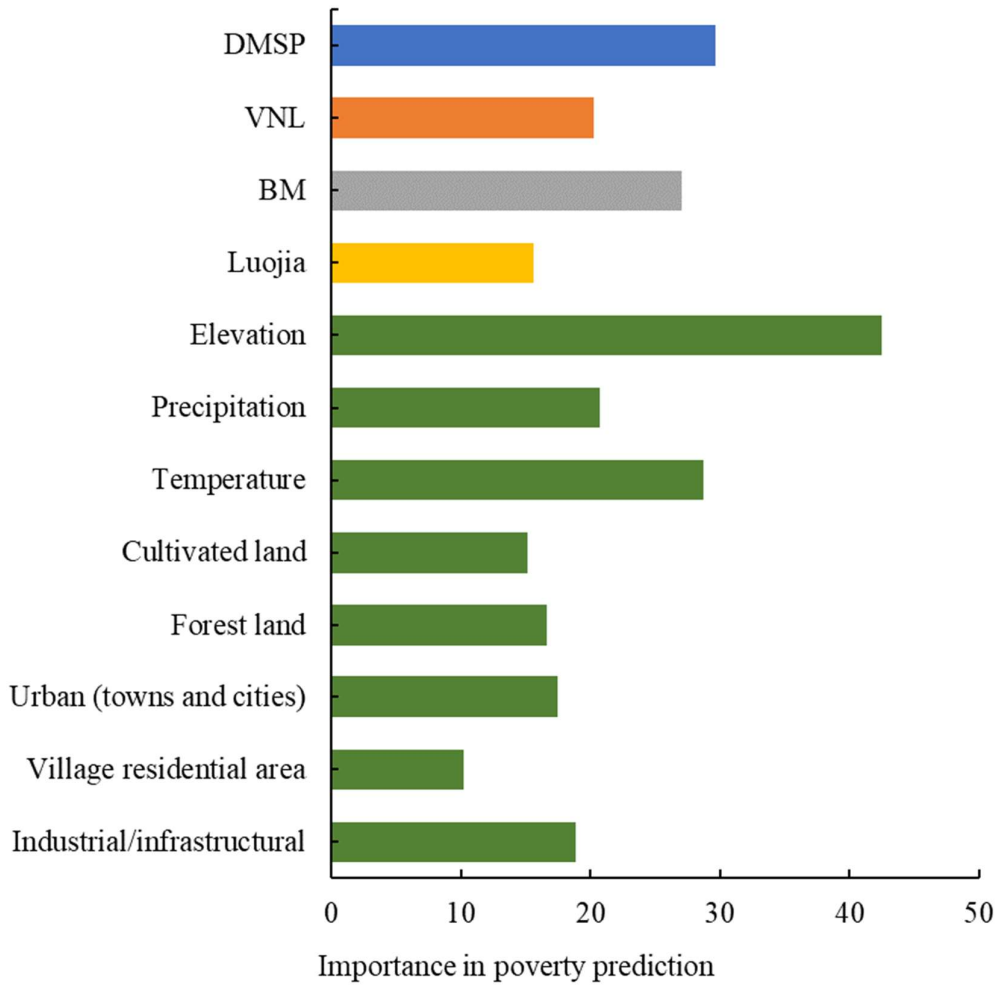
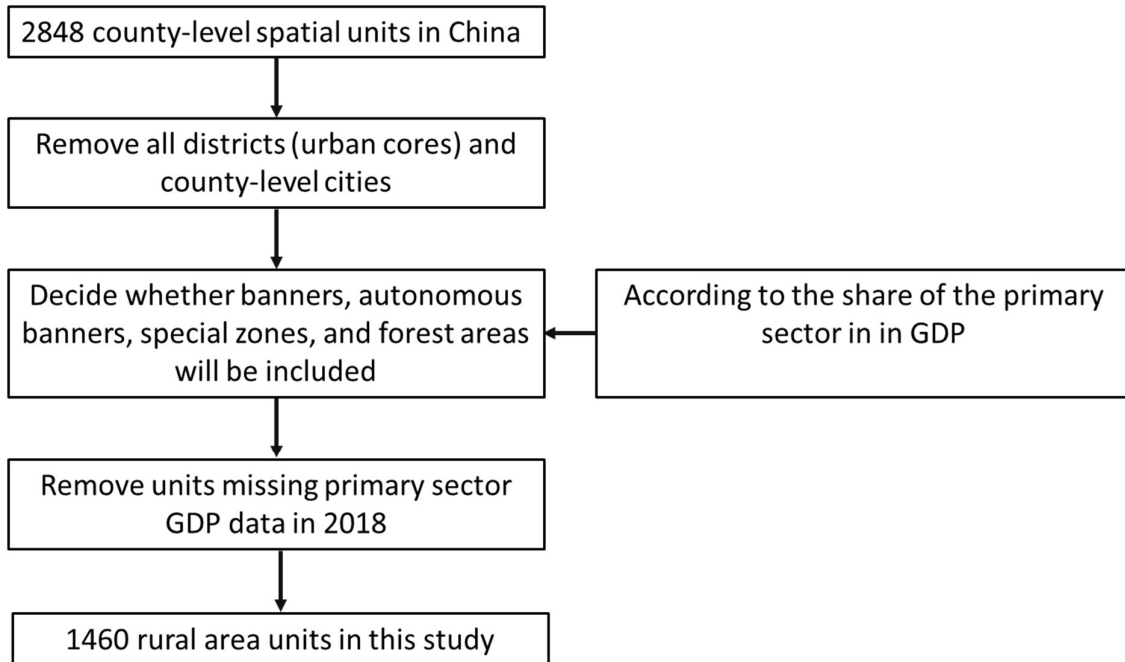


Figure 5. Average contributions of each NTL variable to poverty predictions.
Notes: (a) only includes NTL variables, (b) also includes environmental variables.

Appendix A, Figure 1. Sample selection flowchart



Appendix A, Table 1. Descriptive statistics for outcome variables and luminosity indicators

Variable	<i>County-level</i>		<i>Township-level</i>	
	Mean	Standard deviation	Mean	Standard deviation
ln primary GDP	7.38396	.9856304	/	/
ln fiscal revenue	11.56248	1.077402	/	/
Poverty status	.3958904	.4892087	/	/
Net income per capita	/	/	4384.616	1044.138
Poverty rate	/	/	.3624622	.227051
Electrification rate	/	/	.9859387	.0477137
<i>ln sum of lights</i>				
DMSP	7.911596	1.122323	4.606367	1.665653
VIIRS Night Lights	7.555132	.9481275	4.055358	1.719838
Black Marble	9.927275	1.062219	6.04542	2.006726
Luojia-01	17.61176	.9992102	13.55424	1.353932

Notes: There are n=1460 counties, and n=265 townships.